



Research

Cite this article: Matthews G, Hangartner S, Chapple DG, Connallon T. 2019 Quantifying maladaptation during the evolution of sexual dimorphism. *Proc. R. Soc. B* **286**: 20191372. <http://dx.doi.org/10.1098/rspb.2019.1372>

Received: 12 June 2019

Accepted: 26 July 2019

Subject Category:

Evolution

Subject Areas:

evolution, genetics, theoretical biology

Keywords:

cost of selection, trade-off, cross-sex genetic correlation, sexual antagonism, sexual conflict

Authors for correspondence:

Genevieve Matthews

e-mail: genevieve_matthews@fastmail.fm

Tim Connallon

e-mail: tim.connallon@monash.edu

Electronic supplementary material is available online at <https://dx.doi.org/10.6084/m9.figshare.c.4596245>.

Quantifying maladaptation during the evolution of sexual dimorphism

Genevieve Matthews¹, Sandra Hangartner¹, David G. Chapple¹ and Tim Connallon^{1,2}

¹School of Biological Sciences, and ²Centre for Geometric Biology, Monash University, Clayton, Victoria 3800, Australia

TC, 0000-0002-1962-4951

Females and males have distinct trait optima, resulting in selection for sexual dimorphism. However, most traits have strong cross-sex genetic correlations, which constrain evolutionary divergence between the sexes and lead to protracted periods of maladaptation during the evolution of sexual dimorphism. While such constraints are thought to be costly in terms of individual and population fitness, it remains unclear how severe such costs are likely to be. Building upon classical models for the ‘cost of selection’ in changing environments (*sensu* Haldane), we derived a theoretical expression for the analogous cost of evolving sexual dimorphism; this cost is a simple function of genetic (co)variances of female and male traits and sex differences in trait optima. We then conducted a comprehensive literature search, compiled quantitative genetic data from a diverse set of traits and populations, and used them to quantify costs of sexual dimorphism in the light of our model. For roughly 90% of traits, costs of sexual dimorphism appear to be modest, and comparable to the costs of fixing one or a few beneficial substitutions. For the remaining traits (approx. 10%), sexual dimorphism appears to carry a substantial cost—potentially orders of magnitude greater than costs of selection during adaptation to environmental changes.

1. Introduction

A population’s viability depends upon the extent to which it is adapted to its environment. Nevertheless, maladaptation may arise from several environmental, evolutionary and genetic causes, including deleterious mutations [1,2], maladaptive gene flow that inhibits local adaptation [3,4], and environmental changes that cause an evolutionary mismatch between the population and the environment that it currently inhabits [5–7]. Each of these factors contributes cumulatively to the overall degree of maladaptation of a population, and its extinction susceptibility.

In species with separate sexes, maladaptation can also arise from sex differences in natural selection [8,9]. Because of the different roles that females and males play in reproduction, the sexes have divergent fitness optima for many homologous traits [10]. Sex differences in selection can generate intralocus sexual conflict, in which genetic variation that benefits one sex is deleterious for the other [11,12]. Intralocus sexual conflict may eventually be resolved through the evolution of sexual dimorphism that matches female and male trait expression with the trait optimum of each sex [10,13]. However, the resolution of sexual conflict may be slow, leading to protracted periods of maladaptation during divergence between the sexes [8,12]. Indeed, intralocus sexual conflict will persist whenever sexual dimorphism is underdeveloped, and the sexes remain displaced from their phenotypic optima [9,11,14].

The intensity and duration of intralocus sexual conflict is mediated by the cross-sex genetic correlation (r_{mf}): the additive genetic correlation between homologous male and female traits [8,15,16]. This quantitative genetic parameter describes the degree to which phenotypic effects of genetic variation are correlated between the sexes, which determines the capacity for sexual

dimorphism to evolve. Values of r_{mf} are nearly always positive and are typically large (e.g. $0.8 < r_{mf} < 1$ [15,16]), which implies that the evolution of sexual dimorphism will be constrained for most traits (see [8,17–19]). Although sexual dimorphism can eventually evolve as long as r_{mf} is less than one [8], or other aspects of genetic variance differ between the sexes [20], large values of r_{mf} slow the evolution of sexual dimorphism, and thereby prolong maladaptation during the evolution of each sex to its optimum [8,21].

Two lines of evidence suggest that intralocus sexual conflict contributes to maladaptation [9,12,22] and may thereby dampen population productivity [23,24]. First, phenotypic selection estimates from contemporary animal populations suggest that sexually antagonistic selection occurs in roughly 20% of quantitative traits [11,25], most of which will exhibit strong, positive cross-sex genetic correlations [15]. Multivariate analyses of sex-specific selection reinforce this view, with several studies documenting divergent orientations of directional selection between the sexes [26–29]. Second, estimates of cross-sex genetic correlations for fitness and fitness components are typically weakly positive, or negative, reflecting sex differences in selection on standing genetic variation [15,22,30–32]. However, although these observations imply that sexual conflict contributes to maladaptation, quantifying this contribution remains a formidable challenge.

Here, we develop an approach for indirectly assessing the contribution of intralocus sexual conflict to maladaptation. We first present a quantitative genetic model of maladaptation during the evolution of sexual dimorphism. Our model expands upon Haldane's classical concept of the 'cost of selection' [1,33], in which maladaptation is measured in units of 'selective deaths' (i.e. failure of some individuals to survive and reproduce as a consequence of maladaptation). We show that the cost of evolving sexual dimorphism reduces to a simple function of three measurable population parameters: (i) the cross-sex genetic correlation for each trait (r_{mf}), (ii) the additive genetic variance in each sex, and (iii) the difference between female and male trait optima, which corresponds to the magnitude of sexual dimorphism at equilibrium. We then conducted a comprehensive literature search and compiled data on sexual dimorphism, r_{mf} , and sex-specific additive genetic variation for a large set of traits and animal populations, and used these data to quantify costs of evolving the sexual dimorphism observed in these traits. As we show below, the evolution of sexual dimorphism in some traits appears to come with a substantial long-run cost, yet for most traits, the cost of dimorphism appears to be modest, at least for the traits and populations where data are currently available.

2. Theoretical background

To quantify maladaptation during the evolution of sexual dimorphism, we built upon classical theory for the cost of selection during adaptation to a new environment [1,33,34]. As in previous theory, the cost of selection quantifies the total number of selective deaths that occur during evolution to a genetic or phenotypic optimum (i.e. the cumulative number of individuals that fail to survive or reproduce as a consequence of directional selection to the optimum; see [35]), providing an inclusive measure of maladaptation during single bouts of adaptation. Theoretical formulations

of the cost of selection are appealing from an empirical standpoint because they reduce to simple functions of measurable genetic parameters, including allele frequency shifts across time [1], and estimates of quantitative genetic variances and evolutionary changes in trait means [33,34]. We briefly review this theory before developing a model for the cost of sexual dimorphism and evaluating sex-specific genetic (co)variance data in the light of this theory.

(a) Costs of selection during adaptation to a new environment

Haldane's [1] original formulation of the cost of selection envisioned a population that experienced an abrupt change in its environment, causing genotypes that were common and well adapted in the ancestral environment to become disfavoured in the new one. Maladaptation following an environmental change generates a genetic load, which represents the proportion of individuals in a generation that fails to survive and reproduce as a consequence of maladaptation (i.e. the load t generations after the environmental change is $L_t = (\bar{W}_{\max} - \bar{W}_t) / \bar{W}_{\max}$, where \bar{W}_t is the mean fitness of the population and \bar{W}_{\max} is the mean fitness of a well-adapted population; see [2]). As Haldane emphasized, the genetic load is evolutionarily equivalent to selective culling by animal breeders, which can reduce population size and productivity.

Populations can eventually adapt to a new environment, leading to an increase in the mean fitness and a resolution of the genetic load ($\bar{W}_t \rightarrow \bar{W}_{\max}$ and $L_t \rightarrow 0$). However, the iterated culling process during adaptation results in an accumulation of selective deaths before the load is resolved. Haldane [1] showed that the cumulative load (or 'cost of selection') incurred during substitution of an additive, beneficial allele depends only on its frequency at the time of the environmental change (i.e. q_0 at $t=0$). The cost of the adaptive substitution is

$$C = \int_0^{\infty} \frac{\bar{W}_{\max} - \bar{W}_t}{\bar{W}_{\max}} dt = -2 \ln(q_0), \quad (2.1)$$

which can be substantial. For example, if the favoured allele is initially rare ($q_0 \ll 1$), then the total number of selective deaths required for the allele's substitution can be many times greater than the population's size at any given time. Haldane suggested a typical cost of $C=30$ per substitution, corresponding to $30N$ selective deaths for a population size of N .

Chevin [33] extended Haldane's model to contexts in which quantitative traits evolve towards a phenotypic optimum. Here, the cost of directional selection to the optimum (the cumulative 'lag load') is

$$C = \frac{1}{4} \mathbf{x}_0^T \mathbf{G}^{-1} \mathbf{x}_0, \quad (2.2)$$

where \mathbf{x}_0 is a column vector of initial displacements between trait means and trait-specific optima, \mathbf{G} is the additive genetic variance–covariance matrix for the traits (assumed to be stable over time), and T denotes transposition. For a single trait, $C = (\bar{z}_0 - \theta)^2 (4G)^{-1}$, where \bar{z}_0 is the ancestral trait mean, θ is the trait optimum ($x_0 = \bar{z}_0 - \theta$), and G is the genetic variance of the trait. As in Haldane's model, the cost of selection increases with the initial distance to the optimum.

Costs of selection reflect the inefficiency with which natural selection converts selective deaths into evolutionary progress, which places a limit on the rate of environmental

change that is evolutionarily tolerable [36,37]. Felsenstein [36] reframed Haldane's model by tracking evolutionary and population size dynamics under periodic environmental change. Assuming that each environmental change caused maladaptation at a single locus in the genome, Felsenstein demonstrated that costs of selection will eventually drive a population extinct if the time interval between environmental changes (τ , measured in generations) falls below a critical threshold:

$$\tau_{\text{crit}} = \frac{C}{\ln(1+d)}, \quad (2.3)$$

where C is the cost of selection per substitution, and $1+d$ is the number of offspring per parent at low population densities (d is similar to the intrinsic growth rate of a well-adapted population). Values of d and C may differ among species owing to varying levels of fertility and standing genetic variation, or idiosyncrasies in the nature of selection [34,36,38,39]. However, the bottom line remains the same: the cost of selection sets an upper limit on the tempo of new bouts of selection that a population can tolerate, and this upper limit decreases with increasing C . This reframing of the cost of selection parallels modern evolutionary theories of population persistence, now commonly referred to as 'evolutionary rescue' [40].

(b) Costs of selection during the evolution of sexual dimorphism

Selection for sex differences is notoriously inefficient at yielding an evolutionary response [8,19], providing an arena for large costs of selection during the evolution of sexual dimorphism. While much attention has been directed to costs of selection following environmental changes (see above and [40]), costs of evolving sexual dimorphism have not been explicitly considered by theory, though such costs can be retrieved from straightforward extensions of existing models [33].

Consider an ancestral population that is sexually monomorphic. Following a change in the abiotic, biotic or social environment, female and male phenotypic optima diverge, generating displacements between each sex and its optimum. Following Chevin [33], we assume that fitness in each sex is a Gaussian function of trait expression, genetic variances and covariances are roughly constant over time and abrupt shifts in sex-specific optima initiate each bout of directional selection. Under these conditions, the cumulative sex-averaged cost of directional selection to the optima will be

$$\bar{C} = \frac{C_f + C_m}{2} = \frac{1}{8} \mathbf{x}_{\text{mf},0}^T \mathbf{G}_{\text{mf}}^{-1} \mathbf{x}_{\text{mf},0}, \quad (2.4)$$

(see the electronic supplementary material), where C_f is the female cost, C_m is the male cost, $\mathbf{x}_{\text{mf},0} = (\mathbf{x}_{f,0}, \mathbf{x}_{m,0})^T$ is the vector of initial displacements of female and male trait means from their multivariate trait optima and \mathbf{G}_{mf} is the additive genetic variance–covariance matrix for the set of traits in each sex, i.e. $\mathbf{G}_{\text{mf}} = \frac{1}{2} \begin{pmatrix} \mathbf{G}_f & \mathbf{B} \\ \mathbf{B}^T & \mathbf{G}_m \end{pmatrix}$, where \mathbf{G}_f and \mathbf{G}_m represent the additive genetic variance–covariance matrix for female and male traits, respectively, and \mathbf{B} is the cross-sex additive genetic covariance matrix for the same traits. Equation (2.4) extends equation (2.2) by accounting for sex differences in selection and genetic architecture.

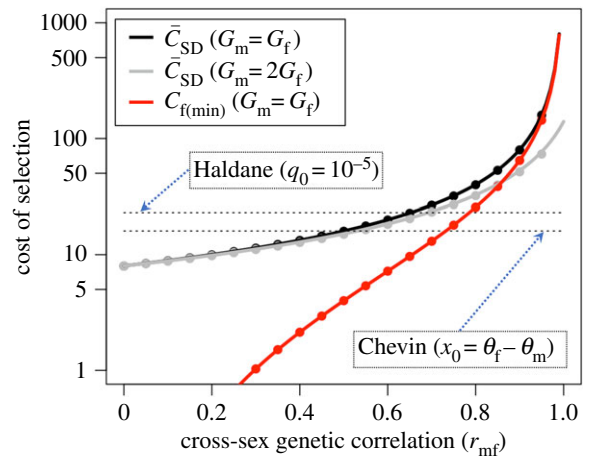


Figure 1. Costs of evolving sexual dimorphism versus classical costs of selection. The solid black and grey curves show the predicted sex-averaged cost of evolving sexual dimorphism, based on equation (2.6). The red curve shows the cost expressed by females based on equation (2.7). Filled circles show deterministic simulation results. The two broken lines show the cost of selection for an adaptive substitution at a single locus (top line: Haldane's model with $q_0 = 10^{-5}$; based on equation (2.1)), or evolution of a quantitative trait to an optimum (bottom line: Chevin's model with $x_0 = (\theta_f - \theta_m)$ and $G = 0.25$; based on equation (2.2)). Aside from Haldane's model, all results use the parameters: $(\theta_f - \theta_m) = 4$ and $(G_f + G_m)/2 = 0.25$; simulations use the additional parameters: $\omega_f^2 = \omega_m^2 = 10^2$ (referring to the curvature of female and male fitness surfaces) and $\sigma = 1$ (referring to the phenotypic variance of the trait). (Online version in colour.)

The sex-averaged cost of directional selection on a single trait towards female and male optima, θ_f and θ_m , is

$$\bar{C} = \frac{(\theta_m - \theta_f)^2 (\bar{G} + r_{\text{mf}} \sqrt{G_f G_m})}{8 G_f G_m (1 - r_{\text{mf}}^2)} + \frac{(\bar{z}_0 - \bar{\theta})(\theta_m - \theta_f)(G_m - G_f) + 2(\bar{z}_0 - \bar{\theta})^2 (\bar{G} - r_{\text{mf}} \sqrt{G_f G_m})}{4 G_f G_m (1 - r_{\text{mf}}^2)}, \quad (2.5)$$

where $\bar{\theta} = (\theta_f + \theta_m)/2$, $\bar{G} = (G_f + G_m)/2$, r_{mf} is the cross-sex genetic correlation for the trait and \bar{z}_0 is the ancestral trait mean. Equation (2.5) captures costs arising from both sexually concordant selection (both sexes selected in the same direction) and selection for sexual dimorphism, of which we are interested in the latter. The minimum of equation (2.5) with respect to \bar{z}_0 provides a baseline cost of selection for sexual dimorphism *per se*, excluding subsidiary costs from sexually concordant selection. This baseline cost of sexual dimorphism is

$$\bar{C}_{\text{SD}} = \frac{(\theta_m - \theta_f)^2}{8(\bar{G} - r_{\text{mf}} \sqrt{G_f G_m})}, \quad (2.6)$$

(see the electronic supplementary material). Figure 1 compares the baseline cost of sexual dimorphism, \bar{C}_{SD} , to classical costs of selection, represented by Haldane's and Chevin's models [1,33]. Costs of sexual dimorphism can be large when the genetic correlation between sexes is strong and positive (i.e. $r_{\text{mf}} > 3/4$, as is typical for morphological traits; [15]), but are comparable to classical costs when genetic correlations are modest ($r_{\text{mf}} < 3/4$). Sex differences in genetic variance dampen \bar{C}_{SD} (figure 1; cf. black and grey curves), though the effect is modest when G_f and G_m are similar in magnitude, as appears to be true for most traits [41].

In most species, males provide less parental investment than females, causing population dynamics to be more tightly coupled to female than to male components of fitness [42,43]. Costs of selection expressed by females may, therefore, provide a more meaningful measure of maladaptation than the sex-averaged costs that we have focused on above. In the electronic supplementary material, we present the costs of directional selection in females and males, individually (i.e. C_f and C_m), for cases where genetic variances and strengths of stabilizing selection are symmetrical between the sexes. From these expressions, the *minimum* cost to females of evolving sexual dimorphism is

$$C_{f(\min)} = \frac{r_{mf}^2(\theta_f - \theta_m)^2}{8G(1 - r_{mf})}, \quad (2.7)$$

(see the electronic supplementary material). When r_{mf} is strongly positive, the minimum cost to females is similar to the sex-averaged cost (figure 1), and otherwise $C_{f(\min)}$ is much smaller than \bar{C}_{SD} . Thus, for traits with a strong genetic correlation between the sexes, females are not spared large costs of selection.

3. Methods

(a) Empirically quantifying costs of evolving sexual dimorphism

For traits that have evolved to their sex-specific optima (i.e. $\bar{z}_f = \theta_f$ and $\bar{z}_m = \theta_m$, where \bar{z}_f and \bar{z}_m are the female and male trait means), our expressions for \bar{C}_{SD} become functions of measurable quantitative genetic parameters. Univariate estimates of G_f , G_m , r_{mf} , \bar{z}_f and \bar{z}_m are available for a wide range of traits and populations [15,41], permitting us to evaluate costs of selection that are consistent with observed magnitudes of sexual dimorphism.

We compiled empirical estimates of G_f , G_m , r_{mf} , \bar{z}_f and \bar{z}_m for a large collection of traits, and used them to parametrize equation (2.6) (see below). In proceeding with our analysis, we made three important assumptions, which we briefly mention here, and return to in the discussion. First, because we lack fitness optimum estimates for any of the traits in the dataset, we assumed that contemporary trait means for each sex have had sufficient time to evolve to the trait optima, in which case estimates of \bar{z}_f and \bar{z}_m can serve as proxies for θ_f and θ_m .

Second, we assumed that contemporary estimates of G_f , G_m and r_{mf} are representative of each trait's (co)variances during its evolutionary history. This is a practical assumption, as historical patterns of G_f , G_m and r_{mf} for a lineage are essentially unmeasurable. Studies of \mathbf{G} matrix stability suggest that this assumption may be reasonable, particularly for highly polygenic traits under weak stabilizing selection, though exceptions have been documented [18,44–46].

Third, our analysis is based on the theoretical model outlined above, which considers costs of selection that follow from a single, abrupt shift in each trait's optimum. As we show further below, costs of selection decrease when shifts in trait optima follow a series of moderate changes rather than a single, large change. Consequently, parametrizations of our model (equations (2.6) and (2.7)) yield upper bounds for \bar{C}_{SD} , representing worst-case scenarios.

(b) Data collection

We searched the literature for studies reporting estimates of the cross-sex genetic correlation (r_{mf}), sex-specific genetic variances or heritabilities (G_f , G_m , h_f^2 , h_m^2), and male and female trait means (\bar{z}_m and \bar{z}_f). We compiled data from two published literature

reviews that focused on subsets of these parameters [15,41], and searched for additional studies by tracking citations of each review and searching Scopus for papers containing combinations of the keywords: 'intersex genetic correlation', 'between-sex correlation', 'between sex correlation', 'cross-sex genetic correlation', 'cross sex genetic correlation', 'quantitative genetics', 'sexual dimorphism' and 'correlation'. Where quantitative genetic parameters were reported for different treatments (e.g. high versus low density), we took the average across the different treatments within each sex. Trait means were averaged across different age groups or populations within the same study if other parameters were only provided once across age groups or populations. For values only reported in figures, we used IMAGEJ (Fiji distribution [47,48]) to extract the quantitative measures for the relevant traits. If heritability (h^2) and phenotypic variance (σ^2) were reported, additive genetic variance was calculated as $G = h^2\sigma^2$. We excluded studies presenting only broad-sense heritability, but included estimates where this was not obvious.

We checked data from 231 relevant studies and excluded 179 that did not contain all parameter estimates. In total, we collected parameter data for 202 traits from 54 studies, spanning 34 species (58 traits were reported in [15]; 60 traits were reported in [41]). We collected standard errors for parameter estimates whenever they were reported, or calculated them when standard deviations and sample sizes were reported. Traits were partitioned into morphological and non-morphological categories, with the latter including behavioural, physiological and developmental traits. Measures of total fitness as the focal trait were removed from our analyses, but fitness components were included. This reduced our final dataset to 196 traits; see the electronic supplementary material, table S1, for the dataset and the full reference list of studies.

(c) Statistical analysis and parametrization of the theoretical model

Prior studies have documented a weak negative correlation between cross-sex genetic correlations (r_{mf}) and magnitudes of sexual dimorphism [15,16], which we tested for in our dataset. We also tested for correlations between sexual dimorphism and additive genetic variation for sexual dimorphism, defined as $V_{SD} = G_f + G_m - 2r_{mf}\sqrt{G_f G_m}$ (i.e. the additive genetic variance for the difference between female and male breeding values). To compare sexual dimorphism across traits, we used the 'sexual dimorphism index' (SDI: the ratio of sex-specific trait means, larger sex divided by smaller sex, minus one; see [15]). To compare genetic variances across traits, we calculated the mean-standardized evolvability of sexual dimorphism:

$$I_{SD} = \frac{V_{SD}}{\bar{z}_{mf}^2} = \frac{G_f + G_m - 2r_{mf}\sqrt{G_f G_m}}{\bar{z}_{mf}^2}, \quad (3.1)$$

where $\bar{z}_{mf} = (\bar{z}_f + \bar{z}_m)/2$ is the sex-averaged mean; such mean-standardization provides an appropriate scale for variance contrasts among traits [49,50]. Spearman's rank correlations were used to quantify associations between: (i) SDI and r_{mf} (as in previous studies [15,16]); and (ii) SDI and I_{SD} . Analyses using Kendall's τ (non-parametric) and Pearson's correlation coefficient (parametric) yielded comparable results.

We took two complementary approaches to evaluate costs of evolving sexual dimorphism with these data. First, for each trait in the dataset, we used parameter point estimates of r_{mf} , G_f , G_m , \bar{z}_m and \bar{z}_f to calculate \bar{C}_{SD} based on equation (2.6), or $C_{f(\min)}$ based on equation (2.7), with \bar{z}_m and \bar{z}_f used as proxies for θ_m and θ_f (see above). However, the use of point estimates of r_{mf} , G_f , G_m , \bar{z}_m and \bar{z}_f can pose problems if there is high uncertainty in the parameter estimates that are fed into the model. For example, point estimates of r_{mf} that are closer to unity than the true value of r_{mf} can yield strongly inflated values of \bar{C}_{SD} . To account for

this issue, we adjusted point estimates of r_{mf} that were greater than 0.95 to $r_{mf} = 0.95$. This upper limit of r_{mf} for calculations of \bar{C}_{SD} yielded results that align well with more rigorous simulation results that take into account uncertainty in parameter estimates (see below).

In our second approach, we used standard errors of parameter estimates to simulate plausible 95% confidence intervals of \bar{C}_{SD} for a reduced set of traits where standard errors were reported for all quantitative genetic parameters ($n = 30$ traits in the reduced trait set). For each trait, we simulated parameters of the theoretical model (i.e. r_{mf} , G_f , G_m , \bar{z}_m and \bar{z}_f) as independent draws from normal distributions with means corresponding to parameter point estimates and standard deviations corresponding to parameter standard errors. Each set of simulated parameter values were used to calculate \bar{C}_{SD} ; this process was repeated 1 million times per trait, resulting in a distribution of \bar{C}_{SD} for each trait that is compatible with the data for that trait. These simulated distributions were used to calculate the mean and 95% confidence intervals of \bar{C}_{SD} for each trait. Simulated values of r_{mf} that fell outside of the biologically plausible range (i.e. $-1 < r_{mf} < 0.99$) were discarded and new values of r_{mf} were drawn; thus, the distribution of simulated r_{mf} values for a trait followed a truncated normal distribution. Likewise, simulated values of G_f and G_m of a trait followed a truncated normal with a lower bound of zero.

We compared \bar{C}_{SD} calculations between trait categories (morphological versus non-morphological) using a generalized linear mixed-effects model (performed with the package MCMCglmm [51]), which accounts for pseudo-replication across studies and species. We constructed our model with study and species as random effects, assuming an exponential distribution for our response variable, and therefore specified the following family argument function: family = 'exponential' [51]. We ran 100 000 iterations with a burn-in of 50 000, a thinning interval of 50 and a parameter expanded prior (residual: $V = 1$, $nu = 0.002$; random effects: $V = 1$, $nu = 1$, $alpha\ mu = 0$, $alpha\ V = 1000$). Auto-correlations (using the autocorr function from the coda package) between the 1000 samples were below the recommended level of 0.1, which determines whether the thinning interval is sufficiently large to prevent autocorrelation, or non-independence, between samples. We inspected plots of traces and posterior distributions to ensure that models converged.

To evaluate effects of species and study on costs of selection, we constructed three additional models, with: (i) only species as a random effect, (ii) only study as a random effect, or (iii) no random effects. We compared the deviance information criterion (DIC) of each model to determine which performed best. All analyses and simulations were conducted using R v. 3.4.2 [52].

4. Results

(a) Genetic correlations, evolvability and the evolution of sexual dimorphism

Consistent with previous studies [15,16], we observed a negative correlation between r_{mf} and the SDI, with the correlation significant for the full dataset and for morphological traits, but not for non-morphological traits (table 1; electronic supplementary material, figure S1). Morphological traits had a higher r_{mf} than non-morphological traits (Wilcoxon's rank-sum test: $W = 1936$, $p = 0.0004$). SDI did not differ significantly between trait categories ($W = 3092.5$, $p = 0.727$).

SDI was positively correlated with mean-standardized evolvability of sexual dimorphism, with significant correlations for the full dataset and for morphological, but not

Table 1. Associations between the SDI and: (i) cross-sex genetic correlations (r_{mf}); or (ii) mean-standardized evolvability of sexual dimorphism (l_{SD} ; see equation (2.8)).

trait category	sample size	correlation	p-value
correlations between SDI and r_{mf}			
all traits	196	-0.24	0.0008
morphological	157	-0.22	0.0057
non-morphological	39	-0.24	0.1455
correlations between SDI and l_{SD}			
all traits	196	0.280	<0.0001
morphological	157	0.333	<0.0001
non-morphological	39	0.181	0.2759

non-morphological, traits (table 1; electronic supplementary material, figure S2). The evolvability of sexual dimorphism was significantly lower for morphological traits than non-morphological traits ($W = 4310$, $p = 2.14 \times 10^{-5}$), reflecting a combination of higher genetic variances and lower genetic correlations in non-morphological traits. These associations between SDI and measures of sex-specific genetic variance (i.e. table 1) imply that either sexual dimorphism evolves more readily in traits with high levels of sex-specific genetic variation, or selection for sexual dimorphism drives the evolution of increased sex-specific genetic variances.

(b) Costs associated with the evolution of sexual dimorphism

Sex-averaged costs of sexual dimorphism— \bar{C}_{SD} from equation (2.6), calculated from point estimates of r_{mf} , G_f , G_m , \bar{z}_m and \bar{z}_f for each trait—spanned a broad range (figure 2; minimum costs to females, based on equation (2.7), are qualitatively indistinguishable; see the electronic supplementary material, figures S3 and S4). While most values were small ($\bar{C}_{SD} < 10$ —i.e. less than 10N total selective deaths—for roughly 60–80% of traits), a subset of traits had very large values ($\bar{C}_{SD} > 100$ for approx. 8–10% of traits). The largest estimated cost among morphological traits was in the order of 10^6 (horn volume in bighorn sheep); the largest among non-morphological traits was in the order of 10^{12} (immunoglobulin levels in bank voles). Many of the highest \bar{C}_{SD} values were associated with traits where sexual dimorphism was extreme, but r_{mf} was not, suggesting that large costs of sexual dimorphism may often arise from large differences between female and male optima rather than strong genetic correlations between the sexes (see the electronic supplementary material, figures S5 and S6). There was no significant effect of study or species on the distribution of \bar{C}_{SD} among trait types according to model DIC values (full model: -9277.647; model with species as a random effect: -9277.893; model with study as a random effect: -9277.242; no random effects model: -9278.49; thus, the model without random effects was most parsimonious, though all DIC values were similar, suggesting that neither of the random effects were particularly important). \bar{C}_{SD} values for morphological traits were greater than those for non-morphological traits (mixed-effects model with random effects excluded: pMCMC = 0.012; model with random effects included: pMCMC = 0.006).

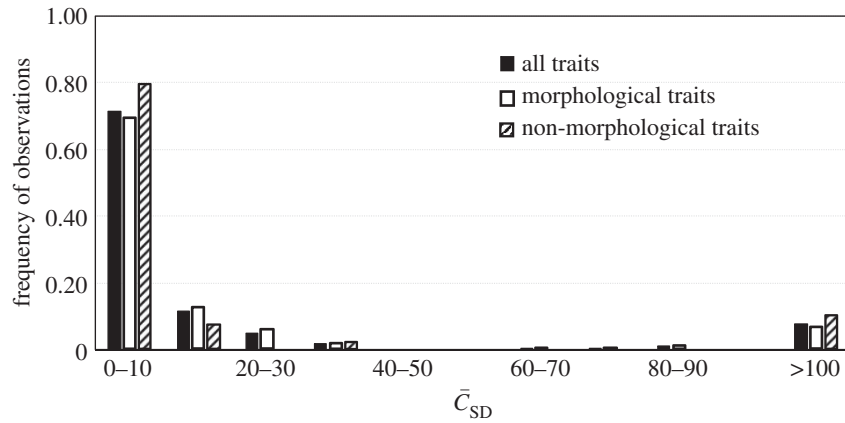


Figure 2. Costs of evolving sexual dimorphism, as calculated from point estimates of quantitative genetics parameters: r_{mf} , G_f , G_m , \bar{z}_m and \bar{z}_f . Results are shown for the entire dataset ($n = 196$ traits), morphological traits ($n = 157$) and non-morphological traits ($n = 39$).

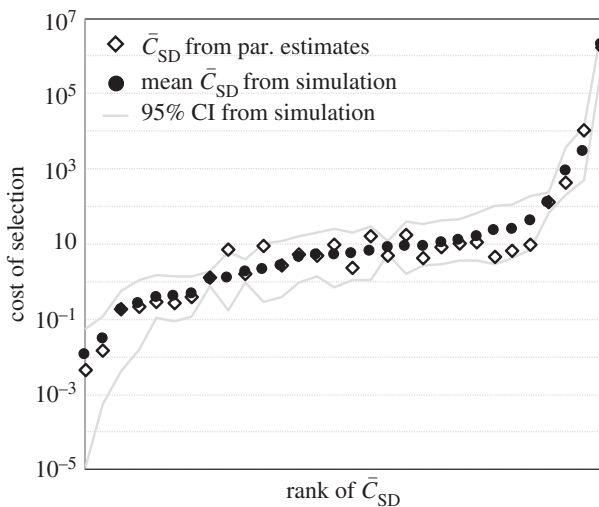


Figure 3. Simulated distributions of the cost of selection, taking into account uncertainty in estimates of r_{mf} , G , \bar{z}_m and \bar{z}_f . Filled circles and lines show means, and upper and lower 95% confidence intervals, respectively, for 30 traits where standard errors of the parameters were reported. For contrast, open diamonds show the estimated values of \bar{C}_{SD} based purely on the point estimates of the parameters (calculated as in figure 2).

Simulations of \bar{C}_{SD} for traits in our reduced dataset (i.e. those where standard errors of parameter estimates were reported) yielded results that were qualitatively similar to the analysis of the full dataset (figure 3). For two-thirds of traits, confidence intervals of \bar{C}_{SD} fell below or overlapped with $\bar{C}_{SD} = 10$ (consistent with the coarser analysis in figure 2), suggesting that sexual dimorphism often carries a modest cost. Ten per cent of traits had costs significantly greater than 100 (lower 95% confidence interval of $\bar{C}_{SD} > 100$).

Costs of sexual dimorphism on the order of 10 or less (approx. 60–80% of traits in our dataset) are equivalent, in Haldane's framework [1] (equation (2.1)), to the cost of a single beneficial substitution with initial allele frequency of $q_0 \approx 0.0067$. Traits within the range of $10 < \bar{C}_{SD} < 100$ are as costly as a small number of adaptive substitutions in Haldane's model (e.g. approx. four substitutions with initial allele frequencies of $q_0 = 10^{-5}$ yield a cost approaching $C = 100$). For the remaining traits in our dataset (approx. 10% of our dataset), costs of sexual dimorphism are orders of magnitude higher than classical costs of selection.

5. Discussion

By extending classical theories for the cost of selection during adaptation to environmental changes [1,7,33,36], we have shown that the baseline cost of evolving sexual dimorphism (as captured by \bar{C}_{SD}) depends upon the balance between: (i) the magnitude of the difference between female and male trait optima (where \bar{C}_{SD} increases with $(\theta_m - \theta_f)^2$), and (ii) the additive genetic variation for sexual dimorphism, defined as $V_{SD} = G_f + G_m - 2r_{mf}\sqrt{G_f G_m}$ (where \bar{C}_{SD} declines with V_{SD}). Our model formalizes how sex-specific components of quantitative trait variability and sex differences in selection interact to shape the long-run fitness consequences of intralocus sexual conflict—from the initiation of conflict to its resolution via evolution of sexual dimorphism.

The theory also provides a formal framework by which sex-specific quantitative genetic data may be used to evaluate costs associated with observed patterns of sexual dimorphism. Our analysis of published estimates of sex-specific trait variability and cross-sex genetic correlations, in the light of the model, suggests that roughly 10% of traits are associated with large costs of selection for sexual dimorphism, with the remainder exhibiting modest to small costs. We stress that these conclusions hinge upon three important, and currently unresolved, assumptions about the evolution of sexually dimorphic traits and pervasiveness of unresolved sexual antagonism. We discuss each assumption and its implications below.

(a) Empirically quantifying costs of evolving sexual dimorphism

Our model provides a basis for quantifying costs of evolving sexual dimorphism, provided three key assumptions are met (briefly outlined above). These assumptions concern: (i) the relationship between trait optima and contemporary trait means, (ii) the evolutionary stability of trait genetic variances and covariances, and (iii) the dynamics of trait optimum changes over time. Violations of each assumption have different implications for the true costs of evolving sexual dimorphism, as the first two are conservative (causing us to underestimate \bar{C}_{SD}), and the last is anti-conservative (causing us to overestimate \bar{C}_{SD}). We evaluate each assumption in turn.

\bar{C}_{SD} is a function of the difference between female and male trait optima, yet direct estimates of trait optima are exceedingly rare. We therefore used estimates of trait sexual dimorphism as

proxies for dimorphism in trait optima, which is reasonable as long as traits in our dataset have had sufficient time to evolve towards equilibrium (i.e. $\bar{z}_f = \theta_f$ and $\bar{z}_m = \theta_m$, as predicted by theory [8]). While a perfect match between trait optima and contemporary trait means seems questionable, a rough correspondence between the two may be likely, provided the onset of selection for sexual dimorphism is not too recent. For example, if selection for sexual dimorphism commenced t generations in the past, then the ratio between phenotypic sexual dimorphism and optimal sexual dimorphism will be

$$\frac{|\bar{z}_m - \bar{z}_f|}{|\theta_m - \theta_f|} \approx 1 - e^{-GS(1-r_{mf})t/2}$$

[21], where S represents the strength of stabilizing selection and G is the additive genetic variance of the trait (G and S are assumed to be the same in each sex). With weak stabilizing selection ($S = 10^{-2}$), modest genetic variance ($G = 0.5$) and a high cross-sex genetic correlation ($r_{mf} = 0.9$), it takes approximately 12 000 generations for the sexes to evolve 95% of the distance to their optima (i.e. $|\bar{z}_m - \bar{z}_f|/|\theta_m - \theta_f| = 0.95$); higher genetic variances, stronger stabilizing selection and weaker genetic correlations shorten the timescale. Such timescales are brief from an evolutionary perspective, and it seems unlikely that selection for sexual dimorphism would have commenced within the last 10 000 generations for many of the traits in our dataset. This view aligns with results from a recent meta-analysis, reporting that contemporary directional selection is typically weak among the roughly 20% of traits that are subject to sexually antagonistic selection [25]. Traits with negligible sexual dimorphism and particularly high genetic correlations (i.e. r_{mf} near one) are perhaps the most likely to have underdeveloped sexual dimorphism. Though dimorphism and r_{mf} are negatively correlated in our dataset (table 1; and see [15,16]), r_{mf} is a poor overall predictor of the degree of sexual dimorphism, and only a small fraction of traits shows extremely low dimorphism and extremely high r_{mf} (see the electronic supplementary material, figure S1). Nevertheless, in cases where sexual dimorphism is underdeveloped relative to dimorphism in optima (i.e. $(\bar{z}_m - \bar{z}_f)^2 < (\theta_m - \theta_f)^2$), our inferred costs of selection will be downwardly biased.

Our analysis also assumed that G_f , G_m and r_{mf} are stable over time—an assumption that is both mathematically convenient and speaks to the nature of empirical data on sex-specific genetic variation (i.e. contemporary estimates of \mathbf{G} are available for many traits; historical estimates of \mathbf{G} are non-existent). Temporally and spatially replicated estimates, while rare, show that genetic variances and covariances are often but not always stable (see [44]), including cases in which sex-specific components of genetic variation have diverged between populations [45,53] (but see [54,55]). It has also been suggested that traits with an evolutionary history of sexually antagonistic selection should evolve decreased cross-sex genetic correlations (decreased r_{mf}) and increased additive genetic variance (higher G_f and G_m) following the evolutionary accumulation of sex-limited loci [8,56,57]. If so, our use of contemporary estimates of r_{mf} , G_f and G_m for sexually dimorphic traits may underestimate \bar{C}_{SD} , though further work is clearly needed to evaluate the evolutionary stability of sex-specific genetic (co)variances, which remains an open question [45,53,54,58].

Finally, our model quantifies costs of selection that arise in response to a single, abrupt shift in sex-specific trait optima. Such costs apply in cases where the contemporary pattern of

sexual dimorphism has evolved in response to a single bout of opposing directional selection between the sexes—an assumption that is certain to be incorrect for many traits (i.e. traits for which the optima have shifted incrementally over time). To evaluate the impact of this assumption, consider an alternative scenario in which a series of modest changes to the optima of a trait generate a cumulative sex difference of $\theta_m - \theta_f$. Assuming that k shifts contribute equally to total divergence between female and male optima (each causing divergence of $(\theta_m - \theta_f)/k$), and sexual dimorphism evolves rapidly relative to the time interval between shifts, then the cumulative cost of evolving sexual dimorphism will be

$$\bar{C}_{SD} = \frac{1}{k} \cdot \frac{(\theta_m - \theta_f)^2}{8(G - r_{mf}\sqrt{G_f G_m})}.$$

Compared to equation (2.6), the total cost of selection declines by a factor of $1/k$. Our previous conclusions remain applicable for 90% of traits in our dataset, which exhibit small-to-moderate costs of selection whether trait optima shift abruptly or by series of smaller shifts. For the remaining 10% of traits, costs of selection may be large, though the severity of these costs may be considerably less than implied by the abrupt change model (equation (2.6)).

(b) Costs of sexual dimorphism and population viability

Unresolved intralocus sexual conflict, by contributing to maladaptation, can potentially dampen population size and productivity [24], and in extreme cases result in extinction [59]. The model presented here quantifies the cumulative cost (in units of selective deaths) of evolving sexual dimorphism in single traits. The impact of such costs on population dynamics will also depend on how commonly selection favours new sexual dimorphisms (i.e. the tempo with which bouts of selection for sexual dimorphism are spaced over time), the fertility of reproducing adults in populations experiencing such costs [1,36] and the degree to which these costs are expressed by females [60–62].

Large costs of selection may be tolerable if they rarely arise (i.e. the environment of selection is relatively stable over time [36]; equation (2.3); but see [63]). Examples of conspicuous sexual dimorphisms are common in nature, suggesting that selection frequently favours evolutionary divergence between the sexes [64,65], though we lack formal estimates of the tempo with which new sexually dimorphic traits are favoured. Such estimates could potentially be inferred by mapping traits onto phylogenies (e.g. [66]) or characterizing divergence rates using fossil data [34,67]. Studies of sex-specific trait diversification, when combined with quantitative genetics analyses of trait evolvability (i.e. from contemporary populations), should provide a more complete picture of the long-run consequences of selection for sexual dimorphism.

High costs of selection are more tolerable in species with high reproductive capacities [36] (equation (2.3)). Our dataset is enriched for vertebrate species (including large terrestrial vertebrates), many of which have relatively low population sizes and fertilities (e.g. far lower than those of insects). Further attention to insect taxa, for which large quantitative genetic experiments are amenable, may reveal that they bear larger average costs of selection than vertebrate taxa. Insect species often show elevated rates of adaptive substitution ([68] and references therein). Perhaps they also exhibit greater sexual

dimorphism relative to the amount of sex-specific genetic variance in their traits.

Finally, in species where females provide most of the parental investment, population viability is less impacted by costs of selection that are primarily borne by males [60–62,69,70]. Although we cannot reliably partition sex-averaged costs into separate female and male components, we have approximated the minimum cost to females of evolving sexual dimorphism (equation (2.7)), and find that these minimum costs remain high for traits with strong cross-sex genetic correlations (figure 1). Parametrization of equation (2.7) with available quantitative genetic data yields qualitatively identical results to our analysis of sex-averaged costs (electronic supplementary material, figures S3 and S4), providing no clear evidence

that costs of selection for sexual dimorphism are likely to be substantially lower for females than males.

Data accessibility. The data on which the results are based appear as the electronic supplementary material.

Authors' contributions. All authors contributed to the conception and development of the project. T.C. developed the model. G.M. and S.H. collected and analysed the data. G.M. and T.C. wrote the manuscript, and all authors contributed to editing it.

Competing interests. We declare we have no competing interests.

Funding. This work was supported by funds from the Australian Research Council (Future Fellowship to T.C.) and the School of Biological Sciences at Monash University.

Acknowledgements. We thank the editors, two anonymous reviewers, and Filip Ruzicka and Akane Uesugi for useful suggestions on an earlier version of the manuscript.

References

- Haldane JBS. 1957 The cost of natural selection. *J. Genet.* **55**, 511–524. (doi:10.1007/BF02984069)
- Agrawal AF, Whitlock MC. 2012 Mutation load: the fitness of individuals in populations where deleterious alleles are abundant. *Annu. Rev. Ecol. Evol. Syst.* **43**, 115–135. (doi:10.1146/annurev-ecolsys-110411-160257)
- Kirkpatrick M, Barton NH. 1997 Evolution of a species' range. *Am. Nat.* **150**, 1–23. (doi:10.1086/286054)
- Bolnick DI, Nosil P. 2007 Natural selection in populations subject to a migration load. *Evolution* **61**, 2229–2243. (doi:10.1111/j.1558-5646.2007.00179.x)
- Fisher RA. 1930 *The genetical theory of natural selection*. Oxford, UK: The Clarendon Press.
- Smith JM. 1976 What determines the rate of evolution? *Am. Nat.* **110**, 331–338. (doi:10.1086/283071)
- Lande R, Shannon S. 1996 The role of genetic variation in adaptation and population persistence in a changing environment. *Evolution* **50**, 434–437. (doi:10.1111/j.1558-5646.1996.tb04504.x)
- Lande R. 1980 Sexual dimorphism, sexual selection, and adaptation in polygenic characters. *Evolution* **34**, 292–305. (doi:10.1111/j.1558-5646.1980.tb04817.x)
- Rowe L, Chenoweth SF, Agrawal AF. 2018 The genomics of sexual conflict. *Am. Nat.* **192**, 274–286. (doi:10.1086/698198)
- Arnqvist G, Rowe L. 2005 *Sexual conflict*. Princeton, NJ: Princeton University Press.
- Cox RM, Calsbeek R. 2009 Sexually antagonistic selection, sexual dimorphism, and the resolution of intralocus sexual conflict. *Am. Nat.* **173**, 176–187. (doi:10.1086/595841)
- Bonduriansky R, Chenoweth SF. 2009 Intralocus sexual conflict. *Trends Ecol. Evol.* **24**, 280–288. (doi:10.1016/j.tree.2008.12.005)
- Stewart AD, Pischedda A, Rice WR. 2010 Resolving intralocus sexual conflict: genetic mechanisms and time frame. *J. Hered.* **101**, S94–S99. (doi:10.1093/jhered/esq011)
- Bedhomme S, Chippindale AK. 2007 Irreconcilable differences: when sexual dimorphism fails to resolve sexual conflict. In *Sex, size and gender roles: evolutionary studies of sexual size dimorphism* (eds DJ Fairbairn, WU Blanckenhorn, T. Székely), pp. 185–194. Oxford, UK: Oxford University Press.
- Poissant J, Wilson AJ, Coltman DW. 2010 Sex-specific genetic variance and the evolution of sexual dimorphism: a systematic review of cross-sex genetic correlations. *Evolution* **64**, 97–107. (doi:10.1111/j.1558-5646.2009.00793.x)
- Griffin RM, Dean R, Grace JL, Rydén P, Friberg U. 2013 The shared genome is a pervasive constraint on the evolution of sex-biased gene expression. *Mol. Biol. Evol.* **30**, 2168–2176. (doi:10.1093/molbev/mst121)
- Reeve J, Fairbairn D. 2001 Predicting the evolution of sexual size dimorphism. *J. Evol. Biol.* **14**, 244–254. (doi:10.1046/j.1420-9101.2001.00276.x)
- Delph LF, Steven JC, Anderson IA, Herlihy CR, Brodie III ED. 2011 Elimination of a genetic correlation between the sexes via artificial correlational selection. *Evolution* **65**, 2872–2880. (doi:10.1111/j.1558-5646.2011.01350.x)
- Stewart AD, Rice WR. 2018 Arrest of sex-specific adaptation during the evolution of sexual dimorphism in *Drosophila*. *Nat. Ecol. Evol.* **2**, 1507–1513. (doi:10.1038/s41559-018-0613-4)
- Wyman MJ, Stinchcombe JR, Rowe L. 2013 A multivariate view of the evolution of sexual dimorphism. *J. Evol. Biol.* **26**, 2070–2080. (doi:10.1111/jeb.12188)
- Connallon T, Hall MD. 2016 Genetic correlations and sex-specific adaptation in changing environments. *Evolution* **70**, 2186–2198. (doi:10.1111/evo.13025)
- Chippindale AK, Gibson JR, Rice WR. 2001 Negative genetic correlation for adult fitness between sexes reveals ontogenetic conflict in *Drosophila*. *Proc. Natl Acad. Sci. USA* **98**, 1671–1675. (doi:10.1073/pnas.98.4.1671)
- Arnqvist G, Tuda M. 2010 Sexual conflict and the gender load: correlated evolution between population fitness and sexual dimorphism in seed beetles. *Proc. R. Soc. B* **277**, 1345–1352. (doi:10.1098/rspb.2009.2026)
- Berger D, Martinossi-Aliliberti I, Grieshop K, Lind MI, Maklakov AA, Arnqvist G. 2016 Intralocus sexual conflict and the tragedy of the commons in seed beetles. *Am. Nat.* **188**, E98–E112. (doi:10.1086/687963)
- Morrissey MB. 2016 Meta-analysis of magnitudes, differences and variation in evolutionary parameters. *J. Evol. Biol.* **29**, 1882–1904. (doi:10.1111/jeb.12950)
- Lewis Z, Wedell N, Hunt J. 2011 Evidence for strong intralocus sexual conflict in the Indian meal moth, *Plodia interpunctella*. *Evolution* **65**, 2085–2097. (doi:10.1111/j.1558-5646.2011.01267.x)
- Gosden TP, Shastri KL, Innocenti P, Chenoweth SF. 2012 The B-matrix harbors significant and sex-specific constraints on the evolution of multicharacter sexual dimorphism. *Evolution* **66**, 2106–2116. (doi:10.1111/j.1558-5646.2012.01579.x)
- Stearns SC, Govindaraju DR, Ewbank D, Byars SG. 2012 Constraints on the coevolution of contemporary human males and females. *Proc. R. Soc. B* **279**, 4836–4844. (doi:10.1098/rspb.2012.2024)
- Poissant J, Morrissey MB, Gosler AG, Slate J, Sheldon BC. 2016 Multivariate selection and intersexual genetic constraints in a wild bird population. *J. Evol. Biol.* **29**, 2022–2035. (doi:10.1111/jeb.12925)
- Delcourt M, Blows MW, Rundle HD. 2009 Sexually antagonistic genetic variance for fitness in an ancestral and a novel environment. *Proc. R. Soc. B* **276**, 2009–2014. (doi:10.1098/rspb.2008.1459)
- Punzalan D, Delcourt M, Rundle HD. 2014 Comparing the intersex genetic correlation for fitness across novel environments in the fruit fly, *Drosophila serrata*. *Heredity* **112**, 143–148. (doi:10.1038/hdy.2013.85)
- Connallon T, Matthews G. 2019 Cross-sex genetic correlations for fitness and fitness components: connecting theoretical predictions to empirical patterns. *Evol. Lett.* **3**, 254–262. (doi:10.1002/evl3.116)
- Chevin LM. 2013 Genetic constraints on adaptation to a changing environment. *Evolution* **67**, 708–721. (doi:10.1111/j.1558-5646.2012.01809.x)

34. Charlesworth B. 1984 The cost of phenotypic evolution. *Paleobiology* **10**, 319–327. (doi:10.1017/S0094837300008290)
35. Crow JF. 1970 Genetic loads and the cost of natural selection. In *Mathematical topics in population genetics* (ed. KI Kojima), pp. 128–177. Berlin, Germany: Springer.
36. Felsenstein J. 1971 On the biological significance of the cost of gene substitution. *Am. Nat.* **105**, 1–11. (doi:10.1086/282698)
37. Charlesworth B. 2017 Haldane and modern evolutionary genetics. *J. Genet.* **96**, 773–782. (doi:10.1007/s12041-017-0833-4)
38. Sved JA. 1968 Possible rates of gene substitution in evolution. *Am. Nat.* **102**, 283–293. (doi:10.1086/282542)
39. Smith JM. 1968 ‘Haldane’s Dilemma’ and the rate of evolution. *Nature* **219**, 1114–1116. (doi:10.1038/2191114a0)
40. Bell G. 2017 Evolutionary rescue. *Annu. Rev. Ecol. Evol. Syst.* **48**, 605–627. (doi:10.1146/annurev-ecolsys-110316-023011)
41. Wyman MJ, Rowe L. 2014 Male bias in distributions of additive genetic, residual, and phenotypic variances of shared traits. *Am. Nat.* **184**, 326–337. (doi:10.1086/677310)
42. Rankin DJ, Kokko H. 2007 Do males matter? The role of males in population dynamics. *Oikos* **116**, 335–348. (doi:10.1111/j.0030-1299.2007.15451.x)
43. Harts AMF, Schwanz LE, Kokko H. 2014 Demography can favour female-advantageous alleles. *Proc. R. Soc. B* **281**, 20140005. (doi:10.1098/rspb.2014.0005)
44. Arnold SJ, Bürger R, Hohenlohe PA, Ajie BC, Jones AG. 2008. Understanding the evolution and stability of the G-matrix. *Evolution* **62**, 2451–2461. (doi:10.1111/j.1558-5646.2008.00472.x)
45. Gosden TP, Chenoweth SF. 2014 The evolutionary stability of cross-sex, cross-trait genetic covariances. *Evolution* **68**, 1687–1697. (doi:10.1111/evo.12398)
46. Uesugi A, Connallon T, Kessler A, Monro K. 2017 Relaxation of herbivore-mediated selection drives the evolution of genetic covariances between plant competitive and defense traits. *Evolution* **71**, 1700–1709. (doi:10.1111/evo.13247)
47. Schindelin J *et al.* 2012 Fiji: an open-source platform for biological-image analysis. *Nat. Methods* **9**, 676–682. (doi:10.1038/nmeth.2019)
48. Rueden CT, Schindelin J, Hiner MC, DeZonia BE, Walter AE, Arena ET, Eliceiri KW. 2017 ImageJ2: ImageJ for the next generation of scientific image data. *BMC Bioinf.* **18**, 529. (doi:10.1186/s12859-017-1934-z)
49. Houle D. 1992 Comparing evolvability and variability of quantitative traits. *Genetics* **130**, 195–204.
50. Hansen TF, Pelabon C, Houle D. 2011 Heritability is not evolvability. *Evol. Biol.* **38**, 258–277. (doi:10.1007/s11692-011-9127-6)
51. Hadfield JD. 2010 MCMC methods for multi-response generalized linear mixed models: the MCMCglmm R package. *J. Stat. Softw.* **33**, 1–22. (doi:10.18637/jss.v033.i02)
52. R Core Team. 2018. *R: a language and environment for statistical computing*. Vienna, Austria: R Foundation for Statistical Computing.
53. Barker BS, Phillips PC, Arnold SJ. 2010 A test of the conjecture that G-matrices are more stable than B-matrices. *Evolution* **64**, 2601–2613. (doi:10.1111/j.1558-5646.2010.01023.x)
54. Hangartner S, Lasne C, Sgrò CM, Connallon T, Monro K. In press. Genetic covariances promote climatic adaptation in Australian *Drosophila*. *Evolution*.
55. Blanckenhorn WU, Llaurens V, Reim C, Teuschl Y, Postma E. 2019 Artificial selection on male size depletes genetic variance but not covariance of life history traits in the yellow dung fly. *bioRxiv*. (doi:10.1101/664326)
56. Lande R. 1987 Genetic correlations between the sexes in the evolution of sexual dimorphism and mating preferences. In *Sexual selection: testing the alternatives* (eds JW Bradbury, MB Andersson), pp. 83–94. Chichester, UK: Wiley.
57. Bonduriansky R, Rowe L. 2005 Intralocus sexual conflict and the genetic architecture of sexually dimorphic traits in *Prochyliza xanthostoma* (Diptera: Piophilidae). *Evolution* **59**, 1965–1975. (doi:10.1111/j.0014-3820.2005.tb01066.x)
58. McGlothlin JW, Cox RM, Brodie ED. 2019 Sex-specific selection and the evolution of between-sex genetic covariance. *J. Hered.* **110**, 422–432. (doi:10.1093/jhered/esz031)
59. Kokko H, Brooks R. 2003 Sexy to die for? Sexual selection and the risk of extinction. *Ann. Zool. Fenn.* **40**, 207–219.
60. Agrawal AF. 2001 Sexual selection and the maintenance of sexual reproduction. *Nature* **411**, 692–695. (doi:10.1038/35079590)
61. Siller S. 2001 Sexual selection and the maintenance of sex. *Nature* **411**, 689. (doi:10.1038/35079578)
62. Whitlock MC, Agrawal AF. 2009 Purging the genome with sexual selection: reducing mutation load through selection on males. *Evolution* **63**, 569–582. (doi:10.1111/j.1558-5646.2008.00558.x)
63. Gomulkiewicz R, Houle D. 2009. Demographic and genetic constraints on evolution. *Am. Nat.* **174**, E218–E229. (doi:10.1086/645086)
64. Darwin C. 1871 *The descent of man and selection in relation to sex*. London, UK: John Murray.
65. Andersson MB. 1994 *Sexual selection*. Princeton, NJ: Princeton University Press.
66. Wiens JJ. 2001 Widespread loss of sexually selected traits: how the peacock lost its spots. *Trends Ecol. Evol.* **16**, 517–523. (doi:10.1016/S0169-5347(01)02217-0)
67. Wright DB. 1993 Evolution of sexually dimorphic characters in peccaries (Mammalia, Tayassuidae). *Paleobiology* **19**, 52–70. (doi:10.1017/S0094837300012318)
68. Gossmann TI, Keightley PD, Eyre-Walker A. 2012 The effect of variation in effective population size on the rate of adaptive molecular evolution in eukaryotes. *Genome Biol. Evol.* **4**, 658–667. (doi:10.1093/gbe/evs027)
69. Mallet MA, Chippindale AK. 2011 Inbreeding reveals stronger net selection on *Drosophila melanogaster* males: implications for mutation load and the fitness of sexual females. *Heredity* **106**, 994–1002. (doi:10.1038/hdy.2010.148)
70. Sharp NP, Agrawal AF. 2013 Male-biased fitness effects of spontaneous mutations in *Drosophila melanogaster*. *Evolution* **67**, 1189–1195. (doi:10.1111/j.1558-5646.2012.01834.x)